SUPPORTING TRAFFIC FLOW MANAGEMENT WITH HIGH-DEFINITION IMAGERY

C. K. Toth[a], D. G-Brzezinska [b], C. Merry [b]

[a]OSU, Center for Mapping, 1216 Kinnear Road, Columbus, OH 43212-1154, USA – toth@cfm.ohio-state.edu
[b]OSU, Department of Civil and Environmental Engineering and Geodetic Science, Columbus, USA

Commission I, WGI/2, I/5 & IC WG II/IV

KEY WORDS: High-Definition imagery, vehicle extraction and tracking, traffic monitoring

ABSTRACT:

Remote sensing has made remarkable developments in recent years. Commercial 1-m satellite imagery has become widely available and quickly captured a considerable segment of the remote sensing imaging market. New sensors, including high-performance digital cameras and LiDAR systems, supported by state-of-the-art GPS/IMU-based direct georeferencing, have completely redefined airborne surveying, signaling the end of an era dominated by large-format analog cameras. These rapid technological advancements have come with the potential to widen the range of applications and to go beyond conventional mapping. This paper discusses some aspects of using high-resolution imagery to support traffic flow monitoring and management. The objective of this ongoing research effort is to assess how moving objects over transportation corridors can be extracted and how their velocity can be estimated.

.

1. INTRODUCTION

The National Consortium for Remote Sensing in Transportation Flows (NCRST-F) was established in 2000, under the joint sponsorship of FDOT and NASA (http://www.ncrst.org/research/ncrst-f/ncrst-f_home.html). It consists of researchers at The Ohio State University, George Mason University and the University of Arizona. The primary goal of the Consortium is to improve the efficiency of the transportation system at the national, state and local levels, by integrating remotely sensed traffic flow data obtained from airborne and/or satellite platforms with traditional data collected from the ground.

The ground-based data commonly available for traffic monitoring (such as detection loops, roadside beacons, travel probes and driver input) are spatially local in nature, while remotely sensed data have the capability of providing spatial scale and network connectivity necessary for supporting effective (and real-time) traffic management. It should be mentioned that in USA only about 25 percent of freeways in urban areas are subject to regular real-time traffic control by classical methods, which certainly indicates a need to implement new tools and methods in order to improve (enable) traffic management. Remote sensing offers unique features for traffic monitoring, such as: (1) sensors are not attached to just one location, (which can, for example, track dangerous cargo or incidents); (2) sensors can be deployed during special events (natural disasters, evacuations, etc.); (3) sensors provide superior spatial resolution; and (4) sensors provide up-to-date traveler information, if applied in real-time.

The major application areas where remote sensing can significantly contribute are (1) highway traffic monitoring and management, and (2) freight and intermodal analysis. The use of remote sensing can enhance the efficiency of many of the present practices used to determine the level of service, vehicle kilometers traveled (VKT), annual average daily traffic (AADT), and vehicle classifications and counts. Remote sensing can also help to determine passenger and freight flows at intermodal centers, and identify congestion points and patterns. Airborne or spaceborne imagery can improve spatial resolution and accuracy and the visualization of traffic flows by the fusion of multisensor databases and hypothesis generation.

It is expected that the use of state-of-the-art imaging sensors in airborne and spaceborne platforms using modern geo-referencing and image processing technologies will enable fast, reliable and accurate data capture for traffic flow information retrieval with high spatial and temporal resolution, supporting in particular:

- Vehicle count/type
- Vehicle velocity and travel time estimation
- Origin-destination flows
- Highway densities (passenger car per unit distance per lane) and exit flow monitoring
- Intersection turning volumes
- Detection of congested/incident areas in real-time to support traffic redirection decision-making
- Platoon dispersion/condensation monitoring (can be effectively accomplished only be remote sensing methods)
- Incident detection and response

2. SENSORS AND PLATFORMS

The major platforms currently used in the NCRST-F research activities are spaceborne and airborne, including fixed-winged aircraft, helicopter, UAV and tethered balloons. The imaging sensors being considered are predominantly frame or line CCD-based digital cameras and scanners, including video cameras and multi/hyperspectral systems. LiDAR installed on airborne platforms is also of great interest (Toth et al., 2003). In this paper, only airborne platforms with frame CCD sensors will be discussed in more detail alongside a brief comparison of spaceborne and airborne platforms with respect to sensor characteristics.

Air- and space-based platforms offer much greater spatial coverage than the ground-based sensors, can access remote segments more readily, and as off-the-road sensors can collect the data more safely and with less traffic disruption.

The use of high-resolution satellite imagery (e.g., IKONOS 1-m data) is especially attractive for traffic monitoring purposes, since the imagery would allow wide spatial coverage unobtainable from ground-based sensors. Airborne sensors, on the other hand, can offer excellent temporal and spatial resolution with relatively large ground coverage (significantly smaller than that of satellite but far better than ground-based sensors). A typical intersection imaged by the IKONOS-2 sensor and a 4K by 4K digital camera is shown in Figure 1; the area coverage of the satellite image is about 400 times larger than that of the airborne images.

a)

b)

Figure 1. 1-m satellite (a) and 15-cm airborne digital camera (b) images.

In order to distinguish major vehicle types, characteristic parameters have to be chosen; here we used a six-parameter representation that includes the size of the vehicle footprint and then four vertical parameters (average height values computed over the four equally sized regions) as shown in Figure 3.

Although the difference in resolution between the two images is striking, there is no difficulty for a human in identifying the vehicles in both images. The automation of the process of vehicle extraction is feasible and usually starts with edge detection, followed by some cleaning and then organizing the edges into rectangular shape objects that can be constrained by true parameters when the image scale is known. There are a variety of methods available with different complexity; a typical solution for vehicle extraction and tracking from airborne video is discussed in (Mirchandani at el., 2003). As an illustration, Figure 2 depicts edges extracted from both images of the intersection.

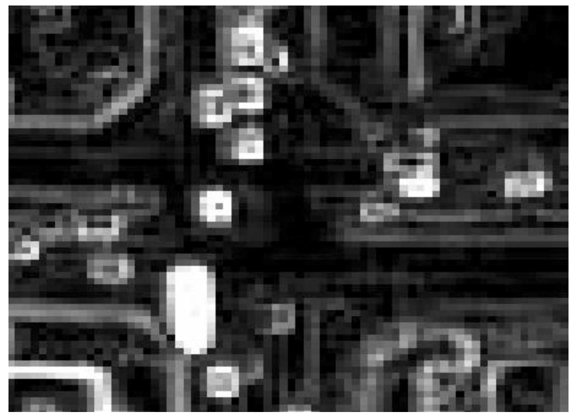

a)

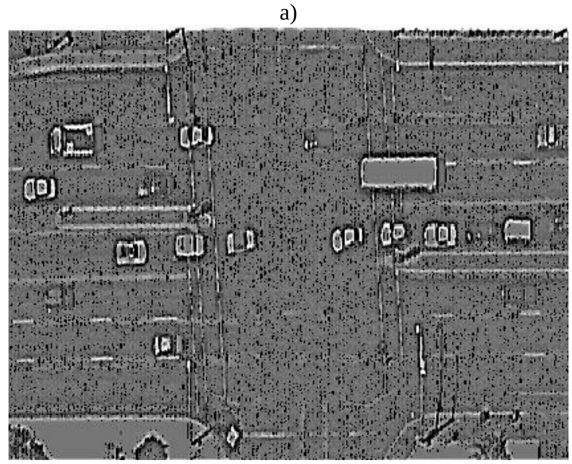

b)

Figure 2. Edges extracted from 1-m satellite (a) and 15-cm airborne (b) images.

Obtaining the number of vehicles and their spatial distribution at a given time is essential for traffic monitoring purposes. More importantly, the changes of that information at a near continuous time scale are of paramount importance as that can describe the entire dynamics of the vehicle traffic. In an extreme scenario, the location of each vehicle in time is perfectly known. Obviously, this cannot be realistically achieved but fortunately there is no need for such a detailed model as mostly the statistics of groups of vehicles are satisfactory for traffic monitoring and management purposes. To obtain this cumulative traffic data, however, vehicles must be tracked at least for a shorter time to estimate their speed and travel directions. Therefore, vehicles must be matched in consecutive images, which is definitely a more complex task than vehicle extraction. Vehicles may have different shapes due to a variety of reasons, may leave and enter the road being monitored, can change lanes and the like. A method, based on edge detection, region filling, rectangular model fitting and template matching is currently under development. In addition, the image difference between consecutive images is used to construct a primary vehicle hypothesis generator. The matching scheme under consideration is based on using existing road geometry information such as road crown lines, centerlines and DEM, and a location prediction from the estimated velocity of the vehicles being tracked. Initial results of the vehicle extraction part are shown in Figure 3.

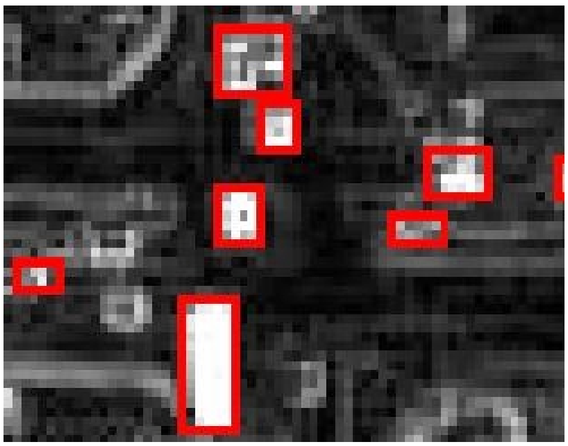

a)

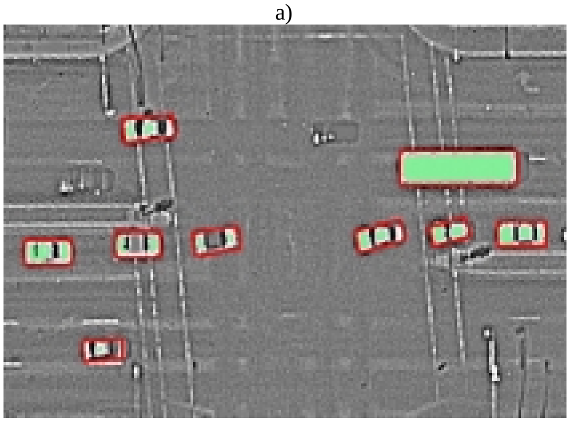

b)

Figure 3. Vehicles extracted from 1-m satellite (a) and 15-cm airborne (b) images.

Clearly, the performance of the vehicle detection is superior for the airborne image; only one vehicle with a very dark tone is missed. The limited resolution of the satellite imagery results in moderate results; there are more missed vehicles as well as objects mistakenly identified as vehicles. Obviously, the low image repetition rate on the satellite platform currently prohibits any type of tracking. Encouraging results that demonstrate that vehicles can indeed be identified and classified accurately from the imagery are in (McCord at al., 2002), which has shown that the numbers of classified vehicles observed in satellite images matching those obtained from ground truth data would demonstrate that vehicles could be counted and classified with reasonable accuracy.

3. TEST DATA ACQUISITION AND PROCESSING

The discussion on platforms and sensors has concluded that long-term statistics are obtainable from satellite imagery but only airborne images can currently offer the potential to extract vehicle speed and consequently traffic flow data in near real-time. Therefore, test flights were arranged to acquire data to perform a feasibility study on the achievable quality of the extracted traffic data. In cooperation between University of Arizona (UoA) and the Ohio State University (OSU), helicopter test flights were arranged to cover a busy highway section, I-10 and major arterial road, Speedway Boulevard in Tucson, AZ. The experimental sensor configuration was based on a 4K by 4K digital camera with a 50 mm focal distance and 15-μm pixel size, 60^2 mm^2 imaging area (Lockheed Martin Fairchild Semiconductors) and a medium/high accuracy IMU (LN100 with raw data output) provided by OSU, and a video and a small resolution digital frame camera assembly provided by UoA. The sensors were placed in the helicopter in the common rigid mount shown in Figure 4. Dual frequency geodetic grade GPS receivers were used to collect carrier phase data, used subsequently in the tightly coupled Kalman filter, processing both raw GPS and IMU data (see, for example, Grejner-Brzezinska, 1999; Toth and Grejner-Brzezinska, 1998). The altitude for the test flights was about 500 m AGL, resulting in ~15 cm ground pixel size. The GPS antenna was rather significantly offset from the rest of the sensors, as it was placed on the helicopter's tail for better signal reception.

Figure 4. Experimental sensor configuration – 4 K by 4K digital camera with IMU and video/digital camera assembly (not visible in this image).

The trajectory of the first May 6th, 2002, flight is shown in Figure 5. The navigation performance error of the GPS/IMU-based system was in the range 2-4 cm (one sigma) for positioning and the attitude data. Image orientation (not including boresight error) was estimated with accuracy (one sigma) of 10-15 arcsec (see Grejner-Brzezinska and Toth, 2002). Six GPS-surveyed control points were used to establish the boresight parameters of the camera systems.

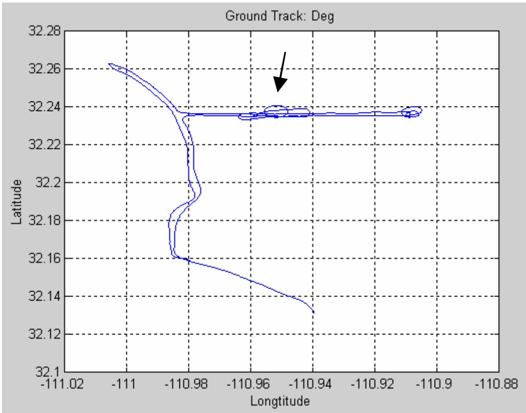

Figure 5. Flight trajectory for the first flight on May 6, 2002.

In our study, a 2-minute data observation period was selected to extract traffic flow data of the intersection of Speedway Boulevard and Euclid Avenue. To facilitate the processing of the images, all the 21 images taken in 6-s intervals were orthorectified using standard 10-m USGS data. Because of the simple road surface geometry and only moderately changing camera position, the rectification produced good starting data for all the vehicle extraction and tracking processes. Figure 6 illustrates the match between two consecutive images using anaglyph coloring; clearly only the moving objects differ in the orthoimage domain. As discussed above, the observed difference between consecutive images is used to create a vehicle hypothesis and thus provides a good support for the process of moving vehicle extraction. Another approach to create a similar "stabilized" image sequence is platform motion correction; a good implementation is reported in (Shastry and Schowengerdt, 2002). Augmenting the sensor suite with LiDAR could not only provide excellent quality DEM but would also add to the robustness of the vehicle extraction and tracking process by providing an excellent three-dimensional description of the vehicles.

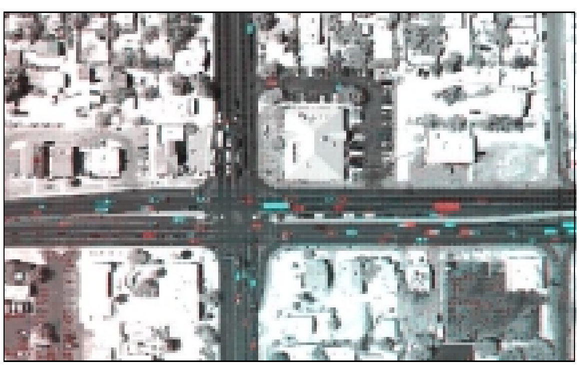

Figure 6. Difference between consecutive orthoimages.

For vehicle classification, three methods have been considered. The main goal here is to classify the vehicles into the given categories: passenger cars (P), multi-purpose vehicles (MPV) and trucks (T). Each category has two subclasses (along and against) considering the traffic direction relative to the flight direction. Therefore, the recognition process is expected to separate the vehicles into six groups, identified as follows:

4. FLOW DATA EXTRACTION

The traffic data extraction from the image sequence was strongly operator-assisted as the vehicle matching procedure under development could not yet deliver satisfactory results. The final output of the processing included a list of all the vehicles passing through the intersection in the given 2-minute interval (144 sec) and each vehicle had its location recorded at the 6-sec sampling rate. The traffic signal had an approximate 1 minute cycle rate (70 sec) and the layout of the intersection is shown in Figure 7. A few representative traffic flow parameters are discussed in the following.

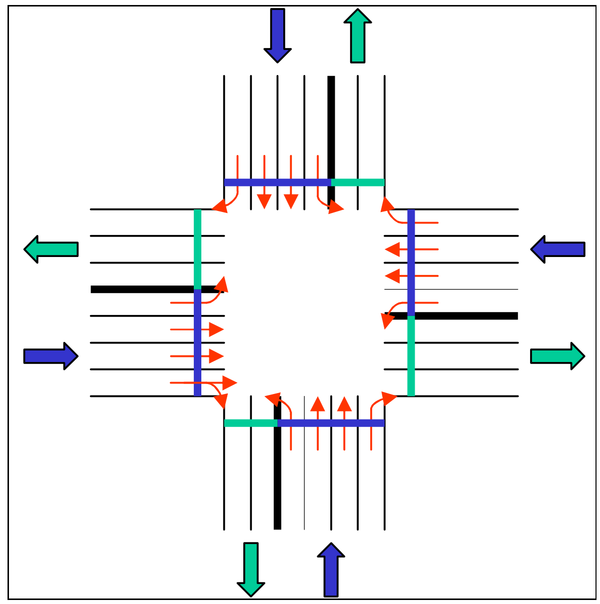

Figure 7. Intersection layout.

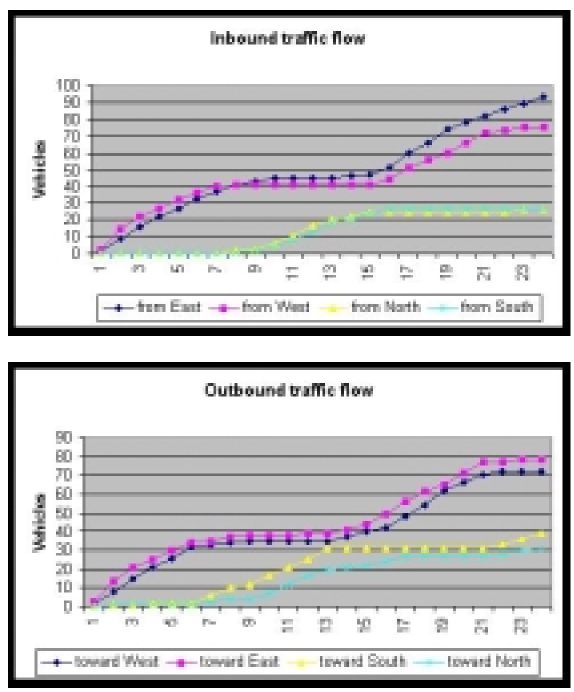

Figure 8. Flow count per traffic light in the four directions.

Frequently used information for traffic management is traffic volume count per traffic light cycle, shown in Figure 8a-b. Divided into the main directions, these measurements provide valuable data for overall traffic dynamics. For instance, it is easy to observe that the Speedway Boulevard (EW) direction carries larger traffic than the Euclid Avenue (NS). A more careful look will reveal that the Speedway direction is losing traffic to Euclid Avenue – turning volume from East to South; the balance flow counts are shown in Figure 9.

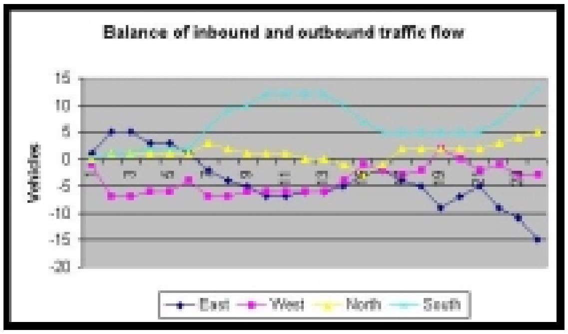

Figure 9. Balance of flow count in the four directions.

More rigorous traffic analysis requires a better temporal representation of the traffic flow compared to the flow data averaged over traffic light cycle rate. For example, individual vehicle velocity profiles are needed to fine-tune the traffic light timing. The limitation of our 4K by 4K digital camera system unfortunately allowed only for a 6-sec image acquisition, which is certainly too low to obtain an adequate sampling of vehicle positions. Nevertheless, a small group of vehicles was tracked and the traveled distance, estimated velocity and acceleration profiles have been estimated. Figure 10 shows the image segments of the tracked vehicle group.

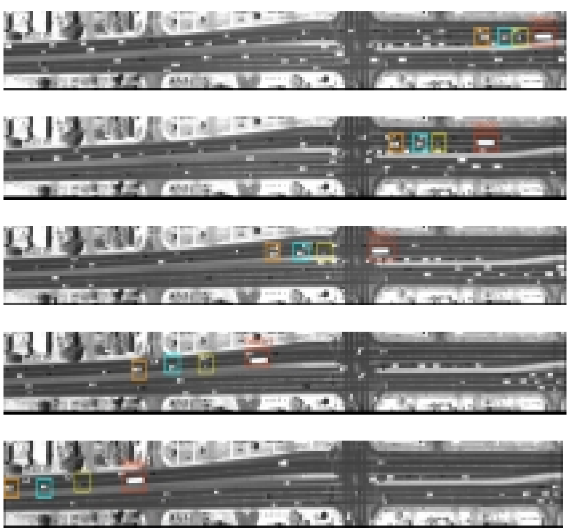

Figure 10. Tracking four moving vehicles.

The traveled distance was modeled by a polynomial function and all the other profiles were derived from the polynomial model. The velocity profiles are shown in Figure 11.

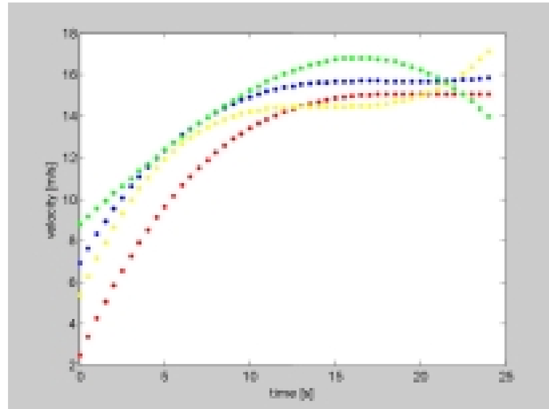

Figure 11. Velocity profile estimates of the four moving vehicles.

5. FLOW DATA QUALITY

The question arises of what is the accuracy of the estimates of the traveled distance and all its derived parameters? There are two aspects to the answer: 1) positioning accuracy of the vehicle position, and 2) temporal resolution (the data rate of the data acquisition) and accuracy. The absolute point positioning accuracy of the experimental airborne sensor suite depends on the georeferencing performance and the imaging system characteristics, including the sensor model and data processing. As discussed earlier the navigation solution, measured in terms of internal error estimation, was excellent in our experiments. Thus the digital camera system modeling errors and the boresighting errors accounted for the most part of the primary error budget. As it is rather difficult to analytically derive the standard deviations of the determined ground coordinates from directly oriented imagery by error propagation, extensive simulations were carried out to assess these accuracy terms, see details in (Csanyi and Toth, 2003). Table 1 shows parameters reflecting the experimental sensor configuration.

Error source	Standard deviation
Image coordinates	± 5µm
Focal length	± 15µm
Principal point	± 15µm
Perspective center position	± 10cm
Attitude angles	± 1’

Table 1. Standard deviation values from simulation.

The RMS values, shown in Table 1 were estimated at the standard Gruber locations.

X [m]	Y_{edge} [m]	Y_{center} [m]	Z [m]
0.28	0.42	0.20	0.65

Table 2. RMS values for ground positioning at 500 m flying height.

As orthophotos were used for all the vehicle extraction and positioning tasks, the impact of the orthorectification process should be also considered. There are two sources of errors: 1) all the image related errors, and 2) the DEM errors. As an older USGS DEM dataset was used, which had been generated from small-scale aerial imagery, only coarse accuracy estimates were available. Therefore, the accuracy of the DEM was randomly checked by models formed from the 4K by 4K images and was found to be about 0.30 m over the road surface. By assuming that the road surface was flat, Kraus' formula (Krauss, 1997) to assess the horizontal errors due to DEM errors was simplified as

$$\sigma_{X,Y} = \frac{\rho'}{c}\sigma_Z$$

where

ΔR	is the horizontal error in the calculated ground position from the orthophoto
c	is the camera focal length
ρ'	is the distance of the image point from the origin of the input image
ΔZ	is the error in the DEM

Since the horizontal ground positioning error caused by the DEM error depends on the distance of the image point from the origin of the input image, one-half of the maximum photo coordinate was considered as a typical value for our investigation, resulting in 0.09 m variance. Thus, the combined effect of the two different error sources, errors related to the original image and errors of the DEM can be calculated as:

$$\sigma_{X,Y} = \sqrt{0.28^2 + 0.09^2} = 0.29m$$

This result was in a good agreement with operator measurements of four control points, which showed about 0.25 - 0.30 m differences. The velocity measurement is based on differencing two location data. Assuming that vehicle location measurements are independent at the two epochs, the variance of the distance difference has a $\sqrt{2}$ times increased variance (0.41 m) with respect to the position measurements. As all sensory data have been precisely time-tagged with a better than 1 ms accuracy, the time measurement error can simply be ignored from our perspective. Thus, the velocity estimates have a less than 0.5 m/s error in the case of the average velocity between the measurement epochs. Obviously, the 6-sec data acquisition rate does not provide an adequate sampling rate to compute instantaneous velocity estimates and if such detailed information is needed, a higher image cycling rate must be used. Normally, the average velocity of many vehicles moving in the same direction is of interest. In this case, the vehicle velocities are averaged and with increasing vehicle numbers, the accuracy of the average velocity estimate will improve ($1/\sqrt{n}$), resulting in excellent flow data in terms of the requirements of traffic monitoring and management.

6. CONCLUSIONS

Our investigations have evidenced that high-definition airborne imagery is an excellent source for obtaining traffic flow data. At 15 cm GSD, vehicles can easily be identified and the large area coverage provides for the simultaneous monitoring of complex traffic scenes. Not only can vehicles be tracked but also the turning volume, velocity and flow can be observed over intersections and interchanges or even over smaller networks of roads. In addition, data that cannot be obtained by loop detectors are easily provided from the high-definition imagery. The performance of the instantaneous vehicle speed estimation is primarily limited by the image acquisition rate, which, at the one frame for every six second rate in our tests, allows only for coarse estimates. Nevertheless, the overall speed of platoons can be derived at good accuracy. Anticipated near-future developments of satellite sensors into the sub-meter range, in particular, in-track high-definition satellite stereo, will likely provide an exceptional source for obtaining traffic flow data over whole cities. The future applicability of the concept depends a lot on how the processes, including navigation and image sequence processing, can be automated and thus performed in real-time or near real-time.

.

7. ACKNOWLEDGEMENTS

This research was partially supported by the NCRST-F program. The IKONOS imagery over Tucson, AZ is courtesy of Space Imaging, LLC, provided through NASA's Earth Science Enterprise Scientific Data Purchase Program, 25 August, 2000. The authors would like to thank Nora Csanyi and Eva Paska, graduate students at the Department of Civil and Environmental Engineering and Geodetic Science, OSU for their help in the data processing.

8. REFERENCES

Csanyi, N. – Toth, C.: (2003): Boresight Misalignment Determination of GPS/INS Supported Camera Systems Using a Single Ground Control Point, Proc. ASPRS Annual Conference, May 5-9, CD-ROM

Grejner-Brzezinska, D. – Toth, C. (2001): Modern Remote Sensing Techniques Supporting Traffic Flow Estimates, ION GPS 2002, Portland, September 24-27, CD-ROM

Grejner-Brzezinska D. A. (1999): Direct Exterior Orientation of Airborne Imagery with GPS/INS System: Performance Analysis, Navigation, Vol. 46, No. 4, pp. 261-270.

Krauss, K., Photogrammetry, Volume 1. (1993): Ferd. Dümmler Verlag, Bonn

McCord, M. – Goel, P. – Jiang, Z. – Coifman, B. – Yang, Y. – Merry, C. (2002): Improving AADT And VDT Estimation With High-Resolution Satellite Imagery, Pecora 15/Land Satellite Information IV/ISPRS Commission I/FIEOS 2002 Conference Proceedings

Mirchandani, P. – Hickman, M. – Angel, A. – Chandnani, D. (2003): Application of Aerial Video for Traffic Flow Monitoring and Management, EOM Vol. 12, No. 4, pp.10-17

Shastry, A. – Schowengerdt, R. (2002): Airborne Video Registration For Visualization And Parameter Estimation Of Traffic Flows, Pecora 15/Land Satellite Information IV/ISPRS Commission I/FIEOS 2002 Conference Proceedings

Toth C. – Grejner-Brzezinska D. – Lovas T. (2003): Traffic Flow Estimates from LiDAR Data, Proc. ASPRS Annual Conference, May 5-9, pp. 203-212, CD-ROM

Toth C. – Grejner-Brzezinska, D. A. (1998): Performance Analysis of the Airborne Integrated Mapping System (AIMS™), ISPRS Commission II Symposium on Data Integration: Systems and Techniques, July 13-17, Cambridge, England, pp. 320-326